IEEE Access
Multidisciplinary | Rapid Review | Open Access Journal

Received August 7, 2019, accepted August 12, 2019, date of publication August 27, 2019, date of current version September 20, 2019.

Digital Object Identifier 10.1109/ACCESS.2019.2937912

Recognition of Aging Stage of Oil–Paper Insulation Based on Surface Enhanced Raman Scattering and Kernel Entropy Component Analysis

DINGKUN YANG[1], WEIGEN CHEN[1], WEIRAN ZHOU[1], JINGXIN ZOU[2], AND ZHOU FAN[3]

[1]State Key Laboratory of Power Transmission Equipment and System Security and New Technology, College of Electrical Engineering, Chongqing University, Chongqing 400044, China
[2]State Grid Chengdu Power Supply Company, Chengdu 610041, China
[3]State Grid Jiangsu Electric Power Engineering Consulting Company Ltd., Nanjing 210000, China

Corresponding author: Weigen Chen (weigench@cqu.edu.cn)

This work was supported in part by the National Science and Technology Project of Power Grid Corp under Grant SGTYHT/16-JS-198, in part by the National Natural Science Foundation of China under Grant 61605020, and in part by the Funds for Innovative Research Groups of China under Grant 51321063.

ABSTRACT This study explores the method of applying surface enhanced Raman scattering (SERS) in diagnosing the aging stage of oil–paper insulation equipment in the power system, which provides access to the on-line mornitoring of electrical equipment. Oil–paper samples in different aging stages were obtained by accelerated aging experiments. Effective Raman signals of insulating oil were collected by using the self-made hexagonal sliver nano-plates SERS substrates and the self-assembled Raman detection platform. For the SERS data of oil-paper insulation samples, kernel entropy component analysis (KECA) was applied to extract the Raman spectral features and support vector machine (SVM) was used to recognize the the aging stage of oil–paper insulation. The results demonstrate that the KECA-SVM method exhibits a good diagnostic capacity and the recognition accuracy of the propsed method reached 81.43 % (57/70). In summary, a new spectral method is proposed to diagnose the aging stage of oil-paper insulation, which lays a foundation for the actual diagnosis of the aging condition in running oil–paper insulation equipment by Raman spectroscopy.

INDEX TERMS Surface enhanced Raman scattering, oil–paper insulation, aging stage, kernel entropy component analysis.

I. INTRODUCTION

The aging of oil–paper insulation is a major and direct hazard to the reliability of electrical equipment like transformer [1]–[3]. During long–term operation, oil-paper insulation inside the transformer gradually degrades under the synergistic effects of thermal, electrical, and chemical factors [4]. Insulation aging causes potential insulation problems and results in failures. Study on the diagnosis of aging conditions is beneficial in maintaining, repairing, or replacing transformers, and is significant to ensure the safety of power systems.

The associate editor coordinating the review of this article and approving it for publication was Jon Atli Benediktsson.

At present, although there are many specific methods for evaluating the aging of oil-paper insulation, such as partial discharge measurement, dielectric response measurement, degree of polymerization (DP) measurement of insulating paper, measurement of dissolved characteristics in oil and so on [5]–[15]. Despite the efforts made by researchers to achieve accurate live aging diagnosis, this work is still a great challenge. There is a lack of a fast comprehensive diagnosis method that contributes to the online mornitoring in this field.

Raman spectroscopy has been widely applied for qualitative or quantitative analysis in many fields, as well as for assessment [16]–[20]. Furfural in oil has been quantitatively analyzed with a detection limit of 14.4 mg/L by a characteristic Raman peak at 1707 cm^{-1} [21]. The further study reached a detection limit of 0.10 mg/L by utilizing extraction

technology [22]. In addition, Raman spectra was used to detect eight typical fault characteristic gases in oil, and the detectability of the system satisfies the requirements of gas diagnosis in power transformer [23]. These studies have proved the feasibility of Raman spectroscopy in condition assessment of power equipment. However, due to the complexity of the oil and the aging process of the oil-paper insulation, it is not reasonable to make a diagnosis based only on the content of few features in the oil. Therefore, though detection of some dissolved features in oil has been achieved, Raman spectra have rarely been used to assess the aging condition of electrical equipment. Previous study [19] has proved the feasibility of Raman spectroscopy in the diagnosis of oil-paper insulation aging. However, the diagnostic accuracy based on principal components analysis (PCA) reached only 73.3% when there were 160 training samples and 105 testing samples. With the vigorous development of algorithm research, the working status of smart grid and many power equipment can be accurately predicted [24]–[29]. However, the researches on the evaluation of oil-paper insulation aging still needs to be improved. With the help of kernel entropy component analysis method, this paper aims to use the Raman spectroscopy to extract more effective spectral characteristics by analyzing the full spectrum of insulating oil which reflects almost all material information, and improve the accuracy of diagnosis.

In this study, to apply the Raman technology into the diagnosis of the aging stage of oil–paper insulation, hexagonal silver nano-plates substrates with high Raman signal enhancement effect, spatial uniformity and high stability in the process of detection were prepared in lab. Oil–paper insulation samples in different aging status were obtained by accelerated thermal aging experiments. Based on observing the change of Raman spectral information entropy in aging process, kernel entropy component analysis was applied to extract spectral features [19]. Finally, a diagnostic model based on support vector machine was established to assess the aging condition of the oil–paper insulation. The flow chart of the whole experiment is shown in Figure 1.

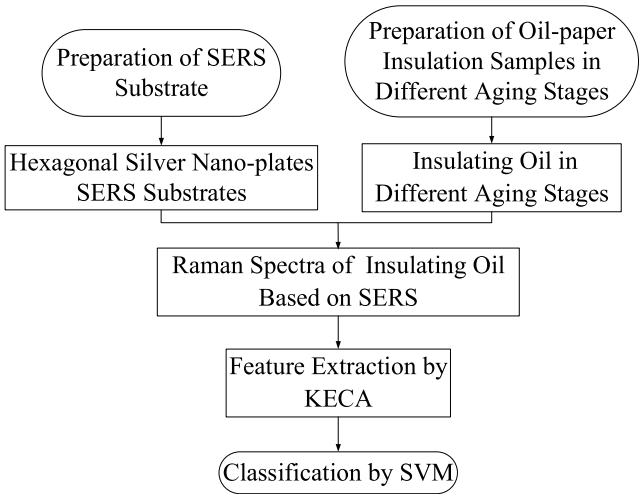

FIGURE 1. The flow chart of the whole experiment.

II. METHODS AND EXPERIMENTS

A. SAMPLE ACQUISITION BY ACCELERATED THERMAL AGING EXPERIMENT

According to the IEEE loading guide [30], we conducted accelerated thermal aging experiments and obtained oil–paper insulation samples at different aging stages in a relatively short period. Karamay 25 # naphthenic mineral oil and kraft paper with the thickness of 0.3 mm were used. The mass ratio of oil to paper is 10:1, which is consistent with the real transformers. Insulating oil and insulating paper are first dried in vacuum drying boxes at 90 °C for 48 h, respectively. Then the paper was immersed in the oil and dried in a vacuum drying box at 90 °C for another 48 h. Meanwhile, copper sheets with dimensions of 50*15*3 mm were added to simulate the copper winding in actual transformers. Finally, 140 samples were placed in aging ovens and heated to 120 °C for the accelerated thermal aging experiment. 20 samples were taken out on days 1, 5, 10, 20, 35, 50, and 80 to obtain the oil–paper insulation samples with different degrees of aging. Half of them were selected as training samples and the other half were used as testing samples.

B. RAMAN DETECTION AND PREPARATION OF SERS SUBSTRATES

To analyze the aging process of the oil-paper insulation, a Raman detection platform was set up to obtain the Raman spectra of the insulating oil. Figure 2 shows the structural chart of the Raman spectrum detection platform.

We used a confocal microscopy to focuse the laser on the surface of substrate in oil to excite Raman scattering. The Raman scattering could be collected by the objective and guided into the charge-coupled device (CCD), which is connected to the spectrometer. The whole system is controlled by a computer. The laser is a 532 nm Cobolt solid-state laser with a maximum power of 500 mW, and the spectrometer is with a blazed grating (600 lines per 600 nm). High spatial resolution 50× long-focal-length objective is used for laser focussing and signal collection. Back thinned CCD (refrigeration temperature: -70 °C, distinguishability: 2000×256, quantum efficiency: $>$ 90 %) is used to obtain high quality spectra. In this experiment, the light intensity on the oil sample is stabilized at 10 mW by a current controller and a temperature controller to prevent the SERS substrate from being damaged by laser and to excite the Raman signal of insulating oil as much as possible. The system can acquire the Raman spectra over the wavenumber range of 400–3200 cm^{-1}. The exposure time and the number of accumulations were set to 10 seconds and 5 times respectively.

Figure 2 also shows the preparation of the hexagonal silver nano-plates surface enhanced substrates. Firstly, the commercial copper foil was cut into square pieces of 0.6*0.6 cm, then immersed in absolute ethanol and deionized

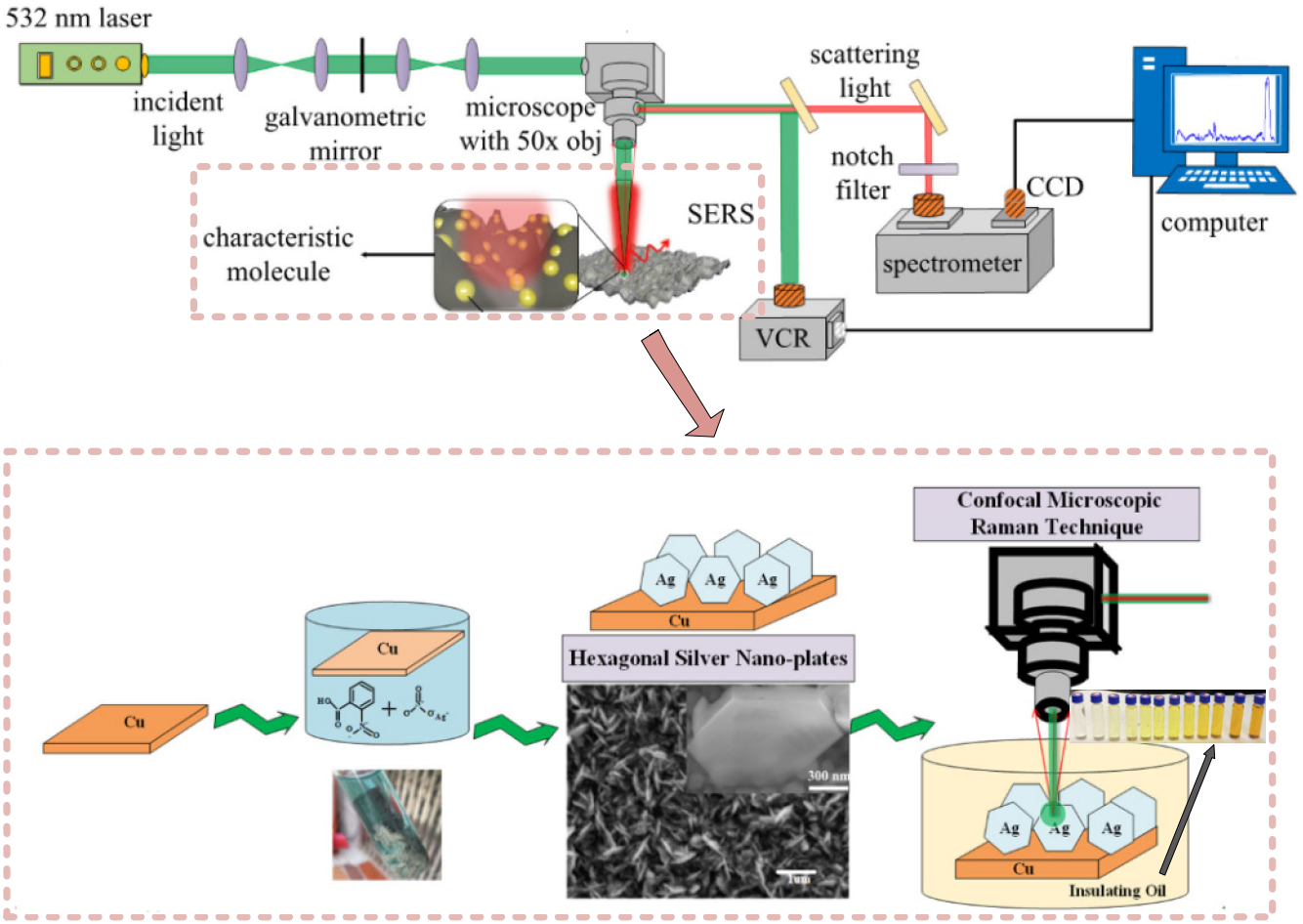

FIGURE 2. The structural chart of the raman spectrum detection platform and the preparation of the SERS substrate.

water respectively, and cleaned in an ultrasonic cleaner for 3 minutes. Secondly, the small cleaned copper sheets are placed in beakers and placed in vacuum drying chambers for drying treatment. Thirdly, the small copper sheets were immersed in 1 mM silver nitrate solution and 1 mM 2-nitrobenzoic acid 200 mL mixed water solution, and the copper sheets were taken out after 4 minutes of reaction. Fourthly, the copper sheets were washed three times with 5 mM copper acetate solution, anhydrous ethanol and deionized water in turn. Finally, the washed copper sheets were dried in a vacuum drying chamber at 50 °C and stored at room temperature. In this way, hexagonal silver nano-plates SERS substrates were obtained. By confocal microscopic Raman technique, the laser is focused on the contact surface accessories between SERS substrate and insulating oil.

C. THE KECA FOR FEATURE EXTRACTION

Wavelet packet decomposition (WPD) provides a time-scale or time-frequency analysis of signals. For Raman spectral data, the word 'time' should be replaced by 'wavenumber' [31]. When the spectra signal s (t) is decomposed by a j-level wavelet packet to obtain 2^j subspaces with equal bangwidth, the sub-signal in each space can be reconstucted as:

$$s_j^n(t) = \sum_k D_k^{j,n} \psi_{j,k}(t) \quad k \in Z \quad n = 0, 1, \cdots, 2^{j-1} - 1 \tag{1}$$

where $D_k^{j,n}$ is the wavelet packet coefficients of the sub-space and $\psi_{j,k}(t)$ is the wavelet function. The energy of the sub-signal can be calculated by:

$$E_n = \sum_k \left| D_k^{j,n} \right|^2 \tag{2}$$

The total energy of s (t) is expressed as the following relation:

$$E = \sum_n E_n \tag{3}$$

$$p_n = E_n / E \tag{4}$$

It indicates the probability distribution of the spectral energy of s (t) in each sub-space. To quantitatively describe the feature information, WPEE is defined as follows based on the

theory of information entropy:

$$WPEE = -\sum_{n} p_n \ln p_n \tag{5}$$

Based on the concept of kernel principal component analysis (KPCA) and Renyi entropy, kernel entropy component analysis (KECA) was proposed to reduce the data dimension and extract Raman spectral features. The original data is projected into the high-dimensional space just as KPCA [32]. KPCA reduce dimensionality by the top eigenvalues and eigenvectors of the kernel matrix. However, the data dimensionality reduction and feature extraction in KECA are obtained by projections onto a subset of Renyi entropy preserving KPCA axes.

As a generalization of information entropy, the Renyi entropy can be expressed as:

$$H(p) = -\log \int p^2(x)\, dx \tag{6}$$

where $p(x)$ is the probability density function generating the data set $D = x_1, \ldots, x_N$. Since the logarithm is a monotonic function, we can focus on the quantity.

$$V(p) = \int p^2(x)\, dx \tag{7}$$

In order to estimate $V(p)$, and then $H(p)$, Parzen window density estimator is employed as:

$$\hat{p}(x) = \frac{1}{N} \sum_{x_t \in D} k_\sigma(x, x_t) \tag{8}$$

where $k_\sigma(x, x_t)$ is the kernel function determined by parameter σ. Using the sample mean approximation of the expectation operator, we can reach that:

$$\hat{V}(p) = \frac{1}{N} \sum_{x_t \in D} \hat{p}(x_t) = \frac{1}{N} \sum_{x_t \in D} \frac{1}{N} \sum_{x_{t'} \in D} k_\sigma(x_t, x_{t'}) = \frac{1}{N} L^T K L \tag{9}$$

where element (t, t') of the $(N \times N)$ kernel matrix K equals $k_\sigma(x, x_t)$ and L is an $(N \times 1)$ vector where each element equals one. Hence, Renyi entropy can be expressed by the eigenvalues and eigenvectors of K. Kernel matrix is eigendecomposed as $K = EDE^T$, thus we have:

$$\hat{V}(p) = \frac{1}{N^2} \sum_{i=1}^{N} \left(\sqrt{\lambda_i} e_{i=1}^T L \right)^2 \tag{10}$$

We descend $\left(\sqrt{\lambda_i} e_{i=1}^T L\right)^2$ to ensure the Renyi entropy of low-dimensional data is similar to the original data. Renyi entropy can be calculated with different σ. In this work, we found that Renyi entropy begin to be stable when the value of σ was close to 3, so the optimal value of σ can be found in the corresponding range.

KECA outputs a new kernel matrix K_{eca} as input space interpretation. K_{eca} is associated with an input space transformation $x \rightarrow x'$ such that the entropy of $x'_1, \ldots, x'_N$ is maximally similar to the entropy of $x_1, \ldots, x_N$.

To sum up, the flow chart of feature extraction using KECA method is shown in Figure 3.

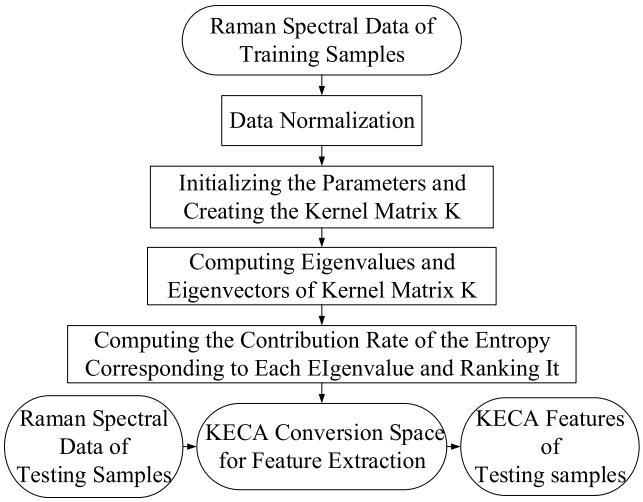

FIGURE 3. The flow chart of feature extraction using KECA method.

D. RECOGNITION OF AGING STAGE OF SAMPLES BASED ON SVM

SVM was first proposed by Cortes and Vapnik in 1995 [33]. It has many unique advantages in solving small sample, non-linear and high-dimensional pattern recognition, and can be extended to other machine learning problems such as function fitting. Based on statistical learning theory and structural risk minimization principle, SVM seeks the best compromise between model complexity and learning ability according to limited sample information in order to obtain the best generalization ability [34], [35].

The period of aging experiment of oil-paper insulation is long, and the number of samples in different aging states can be obtained in one experiment is limited. Therefore, this paper employed SVM to solve the problem of small sample size and identifying the aging stages of the samples.

70 samples were used to train the diagnostic model and the other 70 samples were used for testing. After being scaled to [−1, 1], the feature vectors were loaded to the multi-classification SVM to generate the diagnostic model [36]. The penalty parameter C and kernel parameter γ for SVM in the current study can be optimized by particle swarm optimization (PSO). The best parameters C and γ for SVM can be determined after being trained with the features of the training data.

III. RESULTS AND DISCUSSION

A. SAMPLE ACQUISITION BY ACCELERATED THERMAL AGING EXPERIMENT

By the accelerated thermal aging method described above, we obtained oil-paper insulation samples at different aging times, as shown in Figure 4.

The DP of insulating paper is regarded as one of the best indicators of the aging condition of transformers [30], [37], [38]. It is not feasible to take insulating paper samples from actual transformers, but it is feasible in our

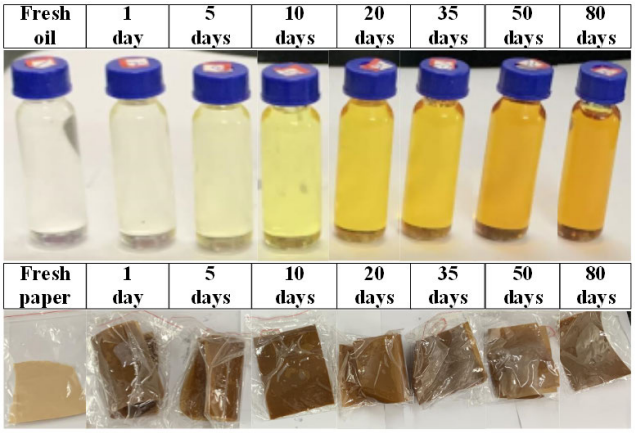

FIGURE 4. Oil-paper insulation samples at different aging times.

experiments. To define the aging stage of the oil–paper insulation, the DP of the insulating paper which was aged with the oil, was measured according to ASTM D4243-99.

Based on the average DP of samples and according to the guide for the diagnosis of insulation aging in oil-immersed power transformers [15], [39], the samples can be divided into four classes that represent the four aging stages: fresh condition (I: DP>900, stage′ 1′, 20 samples), early age (II: 500<DP⩽900, stage′ 2′, 40 samples), medium age (III: 250<DP⩽500, stage′ 3′, 40 samples), and late age (IV: DP⩽250, stage′ 4′, 40 samples).

Table 1 illustrates the changes of DP values of samples with aging time in our experiments. The results showed that our aging experiment accords with the basic aging law.

TABLE 1. The changes of DP values of samples with aging time.

Aging Time	DP	Aging Class
1 day	1075-1260	All in stage I:DP>900
5 days	630-760	All in stage II: 500<DP⩽900
10 days	450-550	Mostly in stage II: 500<DP⩽900
20 days	360-545	Mostly in stage III: 250<DP⩽500,
35 days	245-300	Mostly in stage III: 250<DP⩽500
50 days	190-265	Mostly in stage IV: DP⩽250
80 days	170-203	All in stage IV: DP⩽250

We randomly selected 10 samples from the 20 samples in the stage I, 20 samples from 40 samples in the stage II, 20 samples from 40 samples in the stage III and 20 samples from 40 samples in the stage IV. These 70 samples are used as training samples to ensure samples in each aging stage were used for training the model. The remaining 70 samples are used as test samples.

B. SERS SUBSTRATES

Insulating oil contains thousands of substances, each of which is not particularly abundant. During the aging process of oil-paper insulation, complex chemical reactions will produce a lot of traces of aging products. These traces of aging products are the key to judge the aging status of oil-paper insulation system, but under normal circumstances, their Raman signals are very weak. This makes it difficult to distinguish the Raman signals of samples with different aging degrees. Thus, SERS technique is used to obtain rich spectral information reflecting aging degree. The detection of a large number of samples requires that the SERS substrates have good stability and homogeneity. Hexagonal silver nano-plate arrays were synthesized on the surface of 0.6*0.6 cm copper foil by substitution reaction using silver nitrate solution, which can meet the requirements of aging recognition of oil-paper insulation by Raman spectroscopy. As one of the best substrate materials in surface-enhanced Raman spectroscopy, silver nano-plates have special properties such as surface effect and quantum size effect. Meanwhile, electron migration occurs between copper and silver due to the difference of Fermi level, which inhibits the surface oxidation of silver nanostructures and enhances the stability of SERS substrates. In addition, copper and silver have good heat dissipation performance, which is conducive to Raman detection.

As shown in Figure 5, in order to theoretically analyze the enhancement ability of the prepared SERS substrates, we constructed a model of SERS substrates and simulated the electric field distribution. To analyze stability of the the prepared SERS substrates, we sealed the prepared substrate for 3 days and tested it by the X-ray photoelectron spectroscopy (XPS).

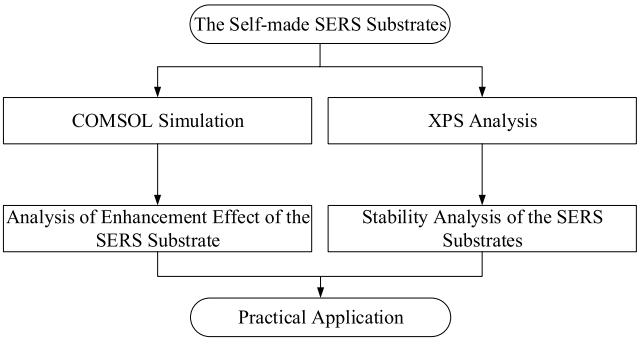

FIGURE 5. Electric field simulation of the silver nanoplates on the self-made SERS substrate.

Based on the surface morphology parameters of copper-based silver nanos-plate SERS substrate, the periodic substrate model of copper-based silver nanosheets was constructed using Radio frequency module of COMSOL software, as shown in Figure 6. With the help of COMSOL, the surface electric field distribution around the substrate surface can be calculated as Figure 7 to characterize the Raman enhancement ability of the SERS substrate.

In the simulation, the periodic unit length is 1400 nm (X-axis direction), the width is 1000 nm (Y-axis direction). The nanoplate was metallic silver and the substrate was metallic copper. The front view (XZ plane) of the silver nanoplate was abstracted as a hexagon with 450 nm edge

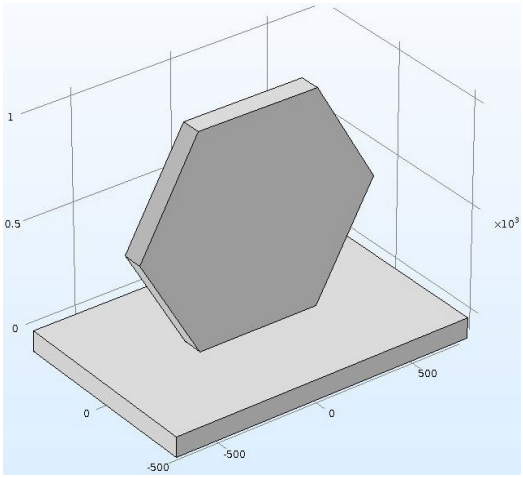

FIGURE 6. The COMSOL model of copper-based silver nanos-plate SERS substrate.

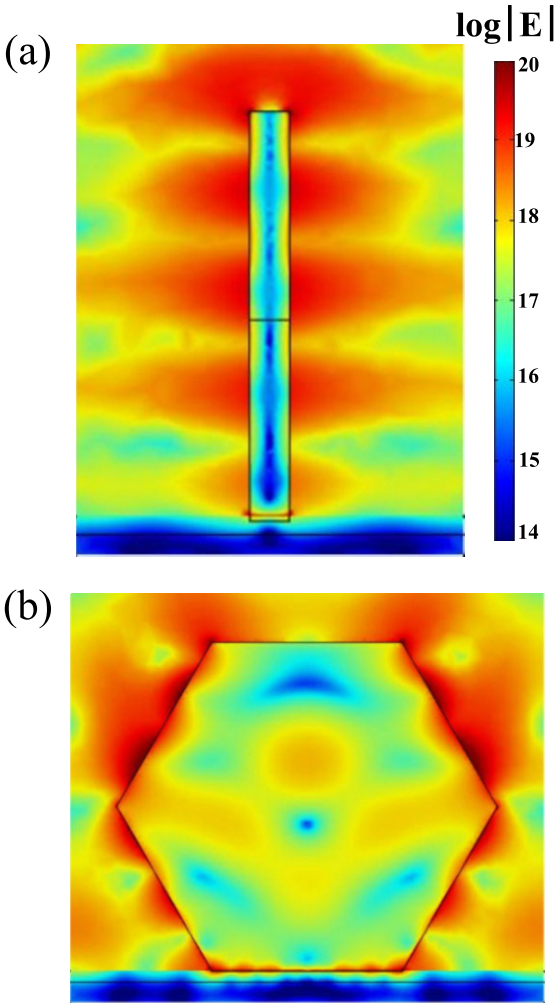

FIGURE 7. Electric field simulation of the silver nanoplates on the self-made SERS substrate.

length (as shown in Figure 7b). The thickness of the silver nanoplate was 80 nm, as shown in Figure 7a (YZ plane). The interval between the silver nanoplate and the copper substrate was set to 3 nm. In addition, the incident light source is selected as 532 nm wavelength laser, the incident direction is Z negative axis, the polarization direction is x positive axis, and the amplitude is 1 V/m.

According to the classical electromagnetic theory, the enhancement of Raman signal mainly comes from the enhancement effect of local electromagnetic field in nano-scale space caused by incident light irradiation on rough metal surface. Raman scattering intensity is closely related to the electric field intensity. For this substrate, except the enhancement came from the surface plasmon resonance (SPR) produced by metal nanostructures under laser irradiation, there are many sharp nanostructures with very small radius of curvature on the rough surface, which can produce strong local electromagnetic field enhancement effect at the tip of the nanostructure. There are obvious hot spots around the corners and sides. The maximum electric field intensity at the tip of the nanoplates reached 20 V/m. Surface enhancement effect is proportional to the fourth power of electric field intensity. Therefore, the silver SERS substrate can enhance the Raman signal of the aging characteristic substances, which is helpful to get useful information from Raman signal of the oil-paper insulation in different aging stages.

Figure 8 shows the XPS analysis on the substrate. Binding energy of Ag (3d5/2) is 368.24 eV in metal silver, while the binding energy of Ag_2O (3d5/2) is 367.3 eV [40]. If silver is oxidized, the binding energy of Ag (3d5/2) should be reduced by 0.94 eV. However, Figure 8a shows that the binding energy of Ag (3d5/2) moved to 368.9 eV. The reason may be that the redistribution of electrons between copper and silver enhances the stability of the system and makes it difficult to be oxidized.

Finally, we applied the prepared SERS substrate to Raman detection. The effect of surface enhancement on the Raman spectra of insulating oil is shown in Figure 9.

Enhancements are concentrated within the blue line (662-2194 cm^{-1}). The main component of insulating oil is organic matter, and its aging products are mainly composed of carbon, hydrogen and oxygen elements. The enhanced Raman bands mainly included the deformation of aromatic ring (662-1050 cm^{-1}), the stretching vibration of C-C (900-1000 cm^{-1}), the stretching vibration of C-O (1000-1250 cm^{-1}), the -CH_2 and -CH_3 deformation (1150-1450 cm^{-1}), the stretching vibration of C=C in aromatic ring (1300-1650 cm^{-1}) and the stretching vibration of C=O (1550-1700 cm^{-1}). The enhanced Raman bands brought us richer aging information.

Raman spectra of insulating oil in different aging stages are shown in Figure 10.

Without SERS, the Raman spectra of insulating oil with different aging times have low discrimination and serious overlap, as shown in Figure 10a. The Raman spectra of insulating oil with different aging times are quite different when the SERS was used, as shown in Figure 10b. However, the variations of Raman spectra of insulating oil

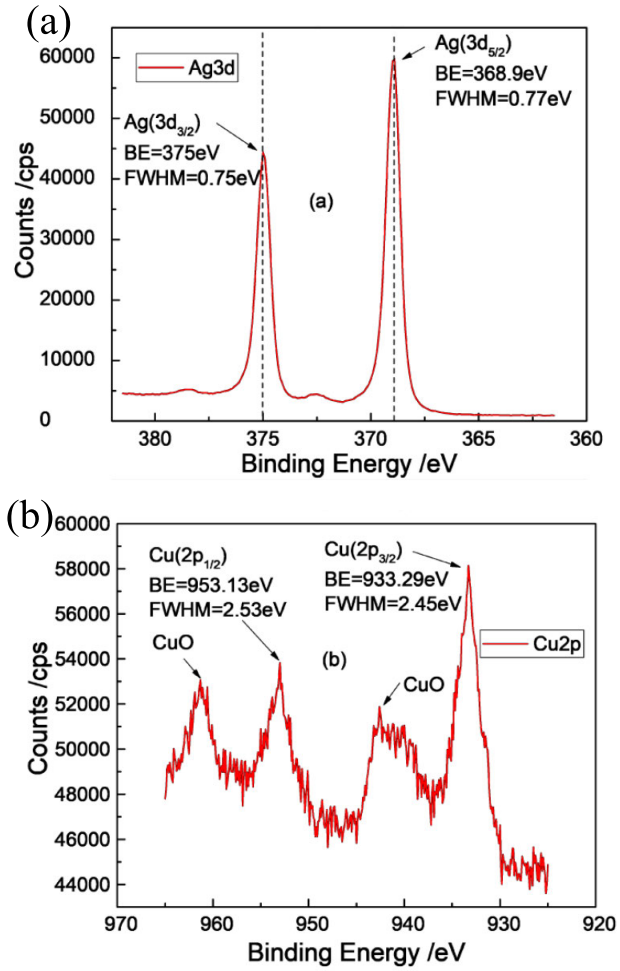

FIGURE 8. The X-ray photoelectron spectra of the substrate.

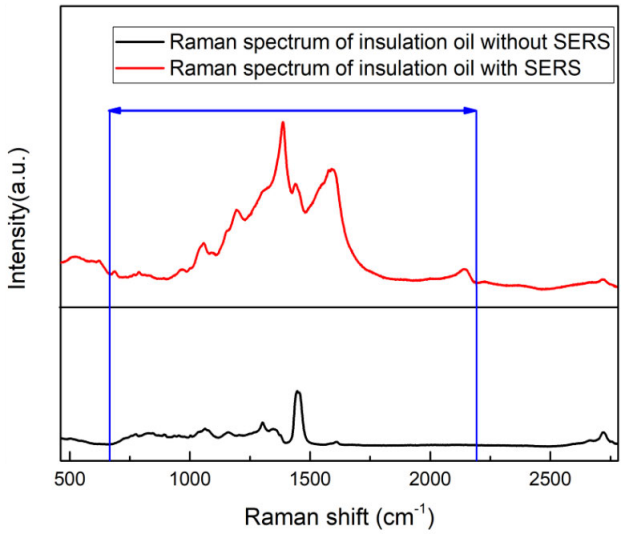

FIGURE 9. The effect of surface enhancement on the raman spectra of insulating oil.

with aging times are very complex, and there is no obvious rule to follow. This is closely related to the complex chemical composition of insulating oil. Insulating oil contain thousands

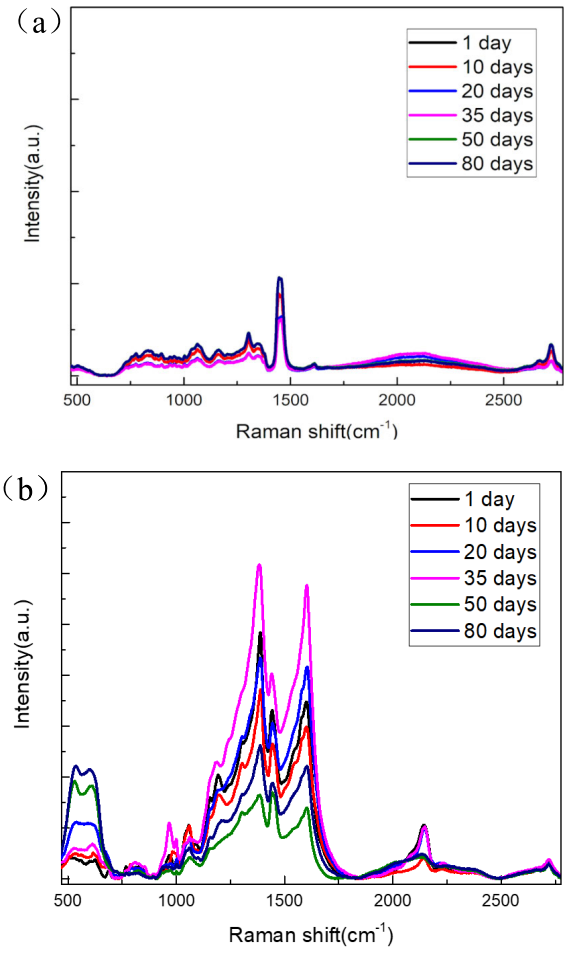

FIGURE 10. (a) Raman spectra of insulating oil with different aging time without SERS. (b) Raman spectra of insulating oil with different aging time with SERS.

of substances, so it is almost impossible to understand all the chemical reactions that occur during aging. We employed the KECA method for feature extraction and the SVM for diagnosis.

The stability testing of the SERS substrate for Raman spectrum detection of insulating oil is shown in Figure 11. The SERS substrate has good stability and repeatability.

C. THE KECA FOR FEATURE EXTRACTION

After arranging the eigenvalues according to the contribution rate of entropy, we take the first nine eigenvalues as the main features extracted by KECA. The i_{th} eigenvector determines the degree to which the i_{th} eigenvalue is affected by the Raman intensity at each location.

Figure 12 shows the first nine eigenvectors of the kernel matrix. As an example, details about the three of the previous nine eigenvectors are shown in Figure 13.

Some relatively high (positive or negative) values were marked and associated with their corresponding variables in the Raman spectra, such as peaks of furfural (1371 cm^{-1}, 1418 cm^{-1}, 1470 cm^{-1} and 1670 cm^{-1}), CO (2144 cm^{-1}), CO_2 (1285 cm^{-1}, 2802 cm^{-1}), methanol (1453 cm^{-1});

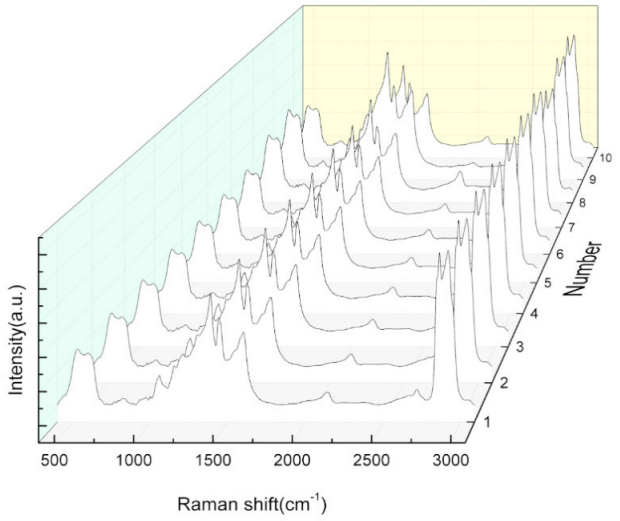

FIGURE 11. The stability tests of the SERS substrate for Raman detection of insulating oil.

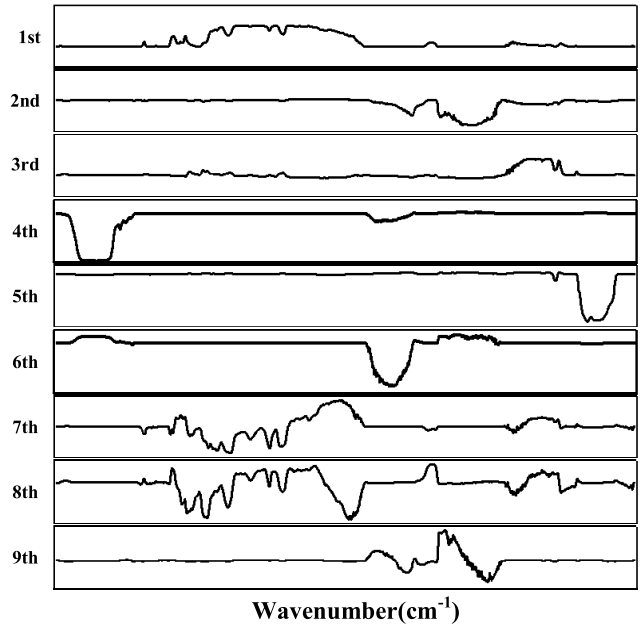

FIGURE 12. Plots of the first nine eigenvectors.

acetone, which is the recently proposed aging characteristic, generated peaks at 939 cm^{-1}, 1211 cm^{-1}, 1712 cm^{-1} and 3080 cm^{-1} [22], [23]. Taking the above characteristic substances as examples, Raman spectroscopy can reflect the state information of oil-paper insulation. In fact, the information that can reflect the aging state in insulating oil should not only be the above characteristic substances. As shown in the Raman spectra of insulating oil, the Raman signals in many bands vary with the aging degree. Therefore, the analysis based on Raman spectroscopy of insulating oil is a comprehensive analysis. The KECA transform space constructed by the eigenvalues and eigenvectors can transform the original data into spectral features.

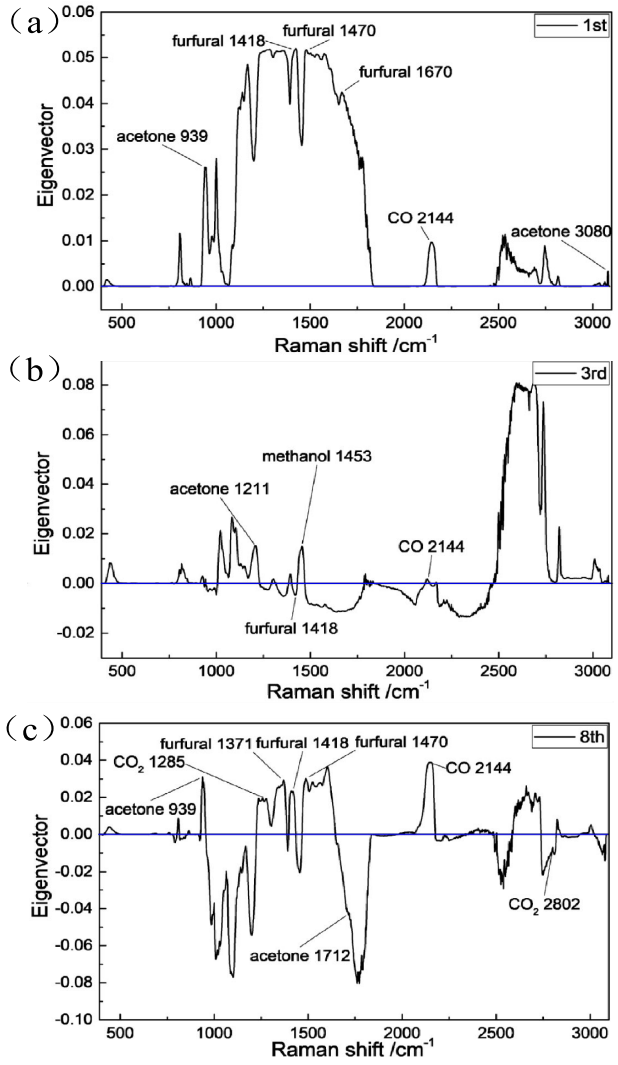

FIGURE 13. Three of the first nine eigenvectors corresponding to the eigenvalues.

Fig. 14 shows the distribution of training sample points when the first three eigenvalues are used to establish a Cartesian space coordinate system.

It is clear that samples of four aging stages have initially become separable. We could imagine that if we use all nine KECA features, the effect will be better. Ultimately, we use all the nine KECA eigenvalues, but the nine-dimensional space created by using nine eigenvalues can not be displayed graphically. We just used SVM to learn 9 KECA eigenvalues of samples in different aging states to build prediction models.

D. RECOGNITION OF AGING STAGE OF SAMPLES BASED ON SVM

After SERS detection of training samples, we analyzed their Raman spectra and obtained their KECA features. With the assistance of SVM method, we correlated these KECA features with the DP values, established an aging diagnosis model, and validated the model. The flow chart is shown in Figure 15.

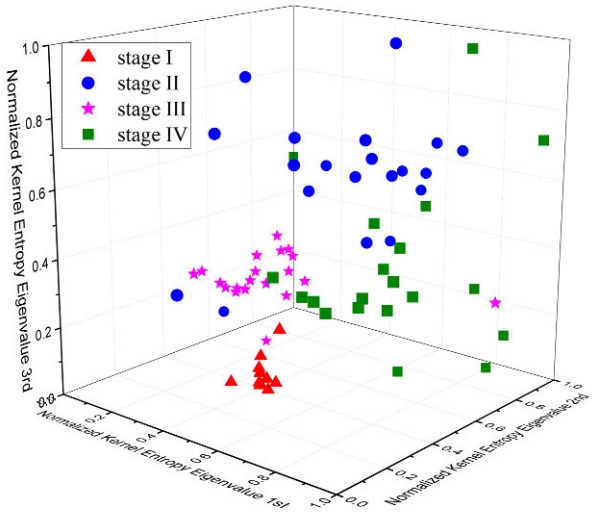

FIGURE 14. Plot of the largest nine entropy terms and the corresponding eigenvalue.

A total of 140 samples were divided into two parts, one for training the KECA-SVM diagnostic model and the other for testing the performance of the model. For training samples, Raman spectral characteristics (KECA features) and aging stages (using DP as the judgment basis) of samples were obtained respectively. Then, with the help of SVM, we analyzed the relationship between the KECA features and the aging stages to established a KECA-SVM diagnostic model. For the testing samples, we also extracted their Raman spectral characteristics (KECA features) and aging stages (using DP as the judgment basis). We input KECA features of test samples into the established KECA-SVM diagnostic model to predict the aging stage of samples, and compared the predicted results with those based on DP tests to verify the accuracy of the model.

As mentioned in section II, the penalty parameter C and kernel parameter γ for SVM are core parameters of the algorithm. The fitness cure of seeking for best C and γ of SVM by PSO is shown in Figure 16a. The best C and γ values for the assessment of transformers were 4.4798 and 0.01, respectively.

Meanwhile, the KECA features of the test samples were calculated on the basis of the transfer matrix of the training samples, thus original data was reduced to nine dimensions and then tested against the discrimination model for classification. The testing results are shown in Table 2 and Figure 16b.

TABLE 2. Actual and predicted results of the test samples by SVM classification using KECA as features.

Actual Aging Stage classified Based on DP	Predicted Stage				Accuracy Rate
	I	II	III	IV	
I	10	0	0	0	100.0%
II	0	14	5	1	70.0%
III	0	0	19	1	95.0%
IV	0	0	4	16	80.0%
Total	(57/70)				81.43%

According to the IEEE loading guide [30], the DP of insulation paper is a widely accepted indicator of the aging condition of transformers. Many researchers used DP value as a reference to judge the degree of aging [5]–[9], [11]. The application of the DP method is limited only in the aging assessment of the actual running equipment, and is not limited in our experiments. Therefore, the diagnostic accuracy of the proposed method in this paper is the diagnostic accuracy compared with the results of the DP method.

The experiment indicated that when the features are extracted by KECA, the PSO-SVM exhibited an accuracy

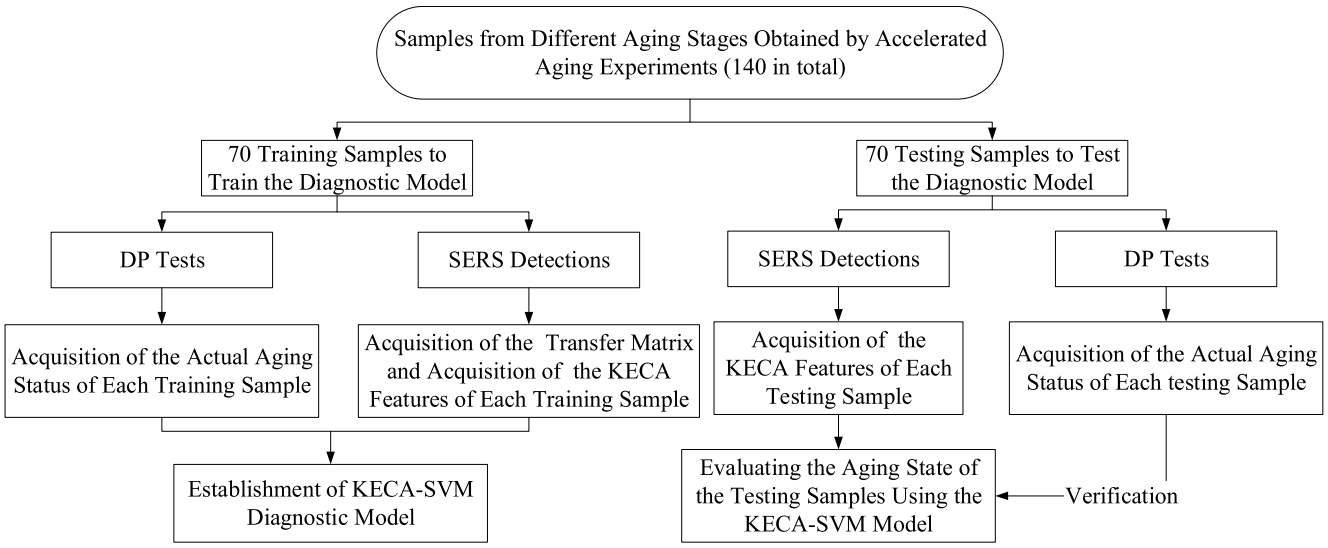

FIGURE 15. Flow chart for establishing and validating the KECA–SVM model.

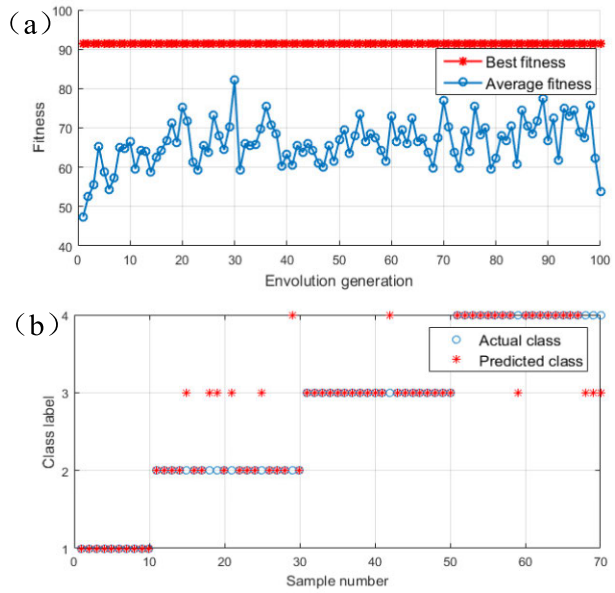

FIGURE 16. (a) The fitness cure of seeking for best C and γ by PSO. (b) Actual and predicted results of the test samples by SVM classification using KECA as features (57/70).

of 81.43 % (57/70) for the test samples. KECA method exhibited a good diagnosis effect on highly aged oil samples but showed slight difficulty with the moderate aging samples. The misclassifications always occurred between the two adjacent aging stages.

The signal of each Raman spectral band includes the vibration information of the characteristic groups in the insulation oil (such as C=O and C=C), which will be generated or changed during the aging process. The spectral changes caused by this situation are complex and non-linear. KECA showed little classification error for the nonadjacent classes, thus avoid severe diagnosis errors because the KECA features, which were extracted from the Raman spectra, has strong nonlinear processing ability for oil samples. Moreover, the aging of oil paper insulation is actually a continuous multi-stage process, so there is no obvious boundary between each aging stage. In addition, affected by the detection error, the aging stage of some samples was hard to identify even by DP. For the reason that we regarded DP as standard, errors in the DP measurement and spectral detection also influenced the accuracy of the testing experiment.

E. COMPARISONS BETWEEN THE PROPOSED METHOD AND OTHER EXISTING METHODS

There are some methods to diagnose the aging of oil-paper insulation at present. However, this work is still worth studying, there are many aspects need to be done better. We compared the proposed method with several existing aging diagnostic methods, as shown in Table 3.

The aging diagnosis method based on furfural content used in [8] showed that there is a linear relationship between DP and the logarithm of furfural content:

$$\log_{10}(c_{furfural}) = 1.56 - 0.0033\ DP \tag{11}$$

where $c_{furfural}$ is the furfural content of oil.

In [8], the R-squared value is 0.8415 when equation (11) was used to predict DP values. This result shows that there is a certain relationship between DP and furfural content, which can be used for aging diagnosis.

The PD method used by Liao Ruijin et al. [5] showed that the diagnostic accuracy of this method reached 82.86% (116/140). In addition, the PD method used in [6] has 80% identification rate to correctly distinguish aging period when 30% noise disturb the original PD signal. The accuracy is satisfactory. However, PD features can be used to assess the insulation aging condition only when PD signals are detectable, and the precondition of PD is the existence of defects in insulation. Therefore, if thermal aging only results in DP decrease of insulation paper, instead of defects and PD, partial discharge analysis will be not suitable [7].

For diagnostic methods based dielectric response, measurements in [9] showed a significant difference between unaged and aged samples, while it failed to isolate samples with different ageing periods. J. Liu *et al.* [11] used frequency dielectric spectroscopy to predict DP, the deviation between the measured DP values and the estimated values were all within 150 when testing 5 samples.

The current study is the first work to use surface enhanced Raman scattering technology on assessing of insulation condition. Raman spectroscopy diagnosis is a new method,

TABLE 3. Comparison of several existing methods.

Method	Number of test samples	Results
Aging diagnosis method based on furfural content used in [8]	not mentioned in [8]	The R-squared value is 0.8415 when equation (11) was used to predict DP values
Partial discharge (PD) method used in [5]	140	82.86% （Compared with the diagnostic method based on DP）
Dielectric response mehod used in [11]	5	wthin 150（Compared with DP values）
The Raman method presented in this paper	70	81.43%（Compared with the diagnostic method based on DP）

which can diagnose rapidly and nondestructively, and has the potential of on-line analysis. However, the weak Raman signal of aging characteristic of oil-paper insulation makes it difficult to apply this method directly. The SERS substrate and the analysis method presented in this paper solved this problem. The diagnostic accuracy of the proposed method in this paper is 81.43%.

This is only a simple comparison which can not show which method is better because:

1) Researchers may use different types of insulating paper and oil when making aging samples.
2) Researchers may have different views on the division of aging stages.
3) In different studies, the number of data used for training diagnostic models and for testing diagnostic models is different.
4) The criteria used to evaluate the quality of various methods may be different.

IV. CONCLUSION

Raman spectroscopy can provide rich information on a system with complex composition. The accuracy rate of the proposed method for diagnosis of the 70 test samples is 81.43%. The results of the study confirmed that SERS technology combined with the concept of information entropy is a promising diagnostic tool to identify the aging stages of oil–paper insulation equipment such as power transformer. The self-made hexagonal silver nano-plates SERS substrate shows its application value in evaluating aging status of oil-paper insulation. In addition to preparation of the SERS substrate, feature extraction of the Raman spectrum is also the key for condition diagnosis. Based on SERS detection, the KECA method was proposed to extracted feature parameter to qualitatively analyze the oil–paper aging stage. The results revealed the high performance of the self-made hexagonal silver nano-plates SERS substrate and that the SERS-KECA is a suitable parameter for classifier meeting the requirement of recognition for fresh condition, early age, medium age, and late age in insulation research. We will further improve the repeatability of SERS substrates and the diagnostic accuracy in future studies. Anyway, the Raman technology with SERS potentially provides a fast, nondestructive, and comprehensive assessment of oil–paper insulation, which is contribute to the on-site and on-line monitoring of oil-paper insulation system.

REFERENCES

[1] R. Liao, J. Hao, G. Chen, and L. Yang, "Quantitative analysis of ageing condition of oil-paper insulation by frequency domain spectroscopy," *IEEE Trans. Dielectr. Electr. Insul.*, vol. 19, no. 3, pp. 821–830, Jun. 2012.

[2] J. Gao, L. Yang, Y. Wang, X. Liu, Y. Lv, and H. Zheng, "Condition diagnosis of transformer oil-paper insulation using dielectric response fingerprint characteristics," *IEEE Trans. Dielectr. Electr. Insul.*, vol. 23, no. 2, pp. 1207–1218, Apr. 2016.

[3] T. K. Saha and P. Purkait, "Investigations of temperature effects on the dielectric response measurements of transformer oil-paper insulation system," *IEEE Trans. Power Del.*, vol. 23, no. 1, pp. 252–260, Jan. 2008.

[4] A. M. Emsley and G. C. Stevens, "Review of chemical indicators of degradation of cellulosic electrical paper insulation in oil-filled transformers," *IEE Proc.-Sci., Meas. Technol.*, vol. 141, no. 5, pp. 324–334, Sep. 1994.

[5] R.-J. Liao, K. Wang, L.-J. Yang, T.-C. Zhou, and S.-X. Zheng, "Study on thermal aging condition assessment of oil-paper insulation based on statistical features of partial discharge," in *Proc. 9th Int. Conf. Properties Appl. Dielectr. Mater.*, Jul. 2009, pp. 325–328.

[6] C.-C. Kuo, "Artificial identification system for transformer insulation aging," *Expert Syst. Appl.*, vol. 37, pp. 4190–4197, Jun. 2010.

[7] R.-J. Liao, L.-J. Yang, J. Li, and S. Grzybowski, "Aging condition assessment of transformer oil-paper insulation model based on partial discharge analysis," *IEEE Trans. Dielectr. Electr. Insul.*, vol. 18, no. 1, pp. 303–311, Feb. 2011.

[8] Y. Lin, L. Yang, R. Liao, W. Sun, and Y. Zhang, "Effect of oil replacement on furfural analysis and aging assessment of power transformers," *IEEE Trans. Dielectr. Electr. Insul.*, vol. 22, no. 5, pp. 2611–2619, Oct. 2015.

[9] T. K. Saha and P. Purkait, "Understanding the impacts of moisture and thermal ageing on transformer's insulation by dielectric response and molecular weight measurements," *IEEE Trans. Dielectr. Electr. Insul.*, vol. 15, no. 2, pp. 568–582, Apr. 2008.

[10] A. Cavallini, G. C. Montanari, and F. Ciani, "Analysis of partial discharge phenomena in paper-oil insulation systems as a basis for risk assessment evaluation," in *Proc. IEEE Int. Conf. Dielectr. Liquids*, Jun./Jul. 2005, pp. 241–244.

[11] J. Liu, X. Fan, H. Zheng, Y. Zhang, C. Zhang, B. Lai, J. Wang, G. Ren, and E. Zhang, "Aging condition assessment of transformer oil-immersed cellulosic insulation based upon the average activation energy method," *Cellulose*, vol. 26, pp. 3891–3908, Apr. 2019.

[12] J. Blennow, C. Ekanayake, K. Walczak, B. Garcia, and S. M. Gubanski, "Field experiences with measurements of dielectric response in frequency domain for power transformer diagnostics," *IEEE Trans. Power Del.*, vol. 21, no. 2, pp. 681–688, Apr. 2006.

[13] T. K. Saha, "Review of modern diagnostic techniques for assessing insulation condition in aged transformers," *IEEE Trans. Dielectr. Electr. Insul.*, vol. 10, no. 5, pp. 903–917, Oct. 2003.

[14] D. H. Shroff and A. W. Stannett, "A review of paper aging in power transformers," *IEE Proc. C-Gener., Transmiss. Distrib.*, vol. 132, no. 6, pp. 312–319, Nov. 1985.

[15] R. J. Liao, Y. Feng, L. J. Yang, B. Xiang, and G. Liu, "Study on generation rate of characteristic products of oil-paper insulation aging," *Proc. CSEE*, vol. 28, no. 10, pp. 142–147, 2008.

[16] H. Lui, J. H. Zhao, D. McLean, and H. S. Zeng, "Real-time Raman spectroscopy for *in vivo* skin cancer diagnosis," *Cancer Res.*, vol. 72, no. 10, pp. 2491–2500, May 15 2012.

[17] A. Bateni, E. Erdem, S. Repp, S. Weber, and M. Somer, "Al-doped MgB_2 materials studied using electron paramagnetic resonance and Raman spectroscopy," *Appl. Phys. Lett.*, vol. 108, no. 20, May 2016, Art. no. 202601.

[18] T. N. K. Zu, A. I. M. Athamneh, E. Collakova, J. Robertson, T. Hawken, C. Aardema, and R. S. Senger, "Assessment of *ex vivo* perfused liver health by Raman spectroscopy," *J. Raman Spectrosc.*, vol. 46, no. 6, pp. 551–558, Jun. 2015.

[19] J. Zou, W. Chen, F. Wan, Z. Fan, and L. Du, "Raman spectral characteristics of oil-paper insulation and its application to ageing stage assessment of oil-immersed transformers," *Energies*, vol. 9, no. 11, p. 946, Nov. 2016.

[20] S. Zong, C. Chen, Z. Wang, Y. Zhang, and Y. Cui, "Surface enhanced Raman scattering based *in situ* hybridization strategy for telomere length assessment," *ACS Nano*, vol. 10, no. 2, pp. 2950–2959, Feb. 2016.

[21] T. Somekawa, M. Fujita, Y. Izawa, M. Kasaoka, and Y. Nagano, "Furfural analysis in transformer oils using laser Raman spectroscopy," *IEEE Trans. Dielectr. Electr. Insul.*, vol. 22, no. 1, pp. 229–231, Feb. 2015.

[22] W. Chen, Z. Gu, J. Zou, F. Wan, and Y. Xiang, "Analysis of furfural dissolved in transformer oil based on confocal laser Raman spectroscopy," *IEEE Trans. Dielectr. Electr. Insul.*, vol. 23, no. 2, pp. 915–921, Apr. 2016.

[23] X. Y. Li, Y. X. Xia, J. M. Huang, and L. Zhan, "A Raman system for multi-gas-species analysis in power transformer," *Appl. Phys. B*, vol. 93, nos. 2–3, pp. 665–669, Nov. 2008.

[24] M. M. Rana, L. Li, S. W. Su, and X. Wei, "Microgrid state estimation: A distributed approach," *IEEE Trans. Ind. Informat.*, vol. 14, no. 8, pp. 3368–3375, 2018.

[25] M. M. Rana, L. Li, and S. W. Su, "An adaptive-then-combine dynamic state estimation considering renewable generations in smart grids," *IEEE J. Sel. Areas Commun.*, vol. 34, no. 12, pp. 3954–3961, Dec. 2016.

[26] M. M. Rana, W. Xiang, and E. Wang, "Smart grid state estimation and stabilisation," *Int. J. Elect. Power Energy Syst.*, vol. 102, pp. 152–159, Nov. 2018.
[27] M. M. Rana, L. Li, and S. W. Su, "Distributed state estimation over unreliable green communication networks with an application to smart grids," *IEEE Trans. Green Commun. Netw.*, vol. 1, no. 1, pp. 89–96, Mar. 2017.
[28] M. M. Rana, L. Li, S. W. Su, and B. J. Choi, "Modelling the interconnected synchronous generators and its state estimations," *IEEE Access*, vol. 6, pp. 36198–36207, 2017.
[29] Y. He, Y. Chen, Z. Yang, H. He, and L. Liu, "A review on the influence of intelligent power consumption technologies on the utilization rate of distribution network equipment," *Protection Control Mod. Power Syst.*, vol. 3, no. 1, p. 18, 2018.
[30] *IEEE Guide for Loading Mineral-Oil-Immersed Transformers and Step-Voltage Regulators-Redline*, IEEE Standard C57.91-2011, 2012.
[31] C. C. Chang and Z. Sun, "Structural damage assessment based on wavelet packet transform," *J. Struct. Eng.*, vol. 128, no. 10, pp. 1354–1361, Oct. 2002.
[32] B. Schölkopf, A. Smola, and K.-R. Müller, "Nonlinear component analysis as a kernel eigenvalue problem," *Neural Comput.*, vol. 10, no. 5, pp. 1299–1319, Jul. 1998.
[33] H. Ankişhan and D. Yılmaz, "Comparison of SVM and ANFIS for snore related sounds classification by using the largest Lyapunov exponent and entropy," *Comput. Math. Methods Med.*, vol. 2013, no. 3, 2013, Art. no. 238937.
[34] Y. Cai, Q. Xie, C. Wang, and F. Lü, "Short-term load forecasting for city holidays based on genetic support vector machines," in *Proc. Int. Conf. Elect. Control Eng.*, 2011, pp. 3144–3147.
[35] X. Deqian, "The research on newly improved bound semi-supervised support vector machine learning algorithm," *Commun. Comput. Inf. Sci.*, vol. 236, pp. 383–390, Jan. 2011.
[36] L. Saidi, J. B. Ali, and F. Fnaiech, "Application of higher order spectral features and support vector machines for bearing faults classification," *ISA Trans.*, vol. 54, pp. 193–206, Jan. 2015.
[37] I. Hohlein and A. J. Kachler, "Aging of cellulose at transformer service temperatures. Part 2. Influence of moisture and temperature on degree of polymerization and formation of furanic compounds in free-breathing systems," *IEEE Elect. Insul. Mag.*, vol. 21, no. 5, pp. 20–24, Sep. 2005.
[38] Y. Wang, Z. Huan, and J. Zhang, "Expediting cellulose insulation aging evaluation and life prediction through degree of polymerization measurements," in *Proc. Int. Conf. Properties Appl. Dielectr. Mater.*, 1988, pp. 328–331.
[39] J. P. V. Bolhuis, E. Gulski, and J. J. Smit, "Monitoring and diagnostic of transformer solid insulation," *IEEE Trans. Power Del.*, vol. 17, no. 2, pp. 528–536, Apr. 2002.
[40] B. V. Crist, *Handbook of Monochromatic XPS Spectra: The Elements of Native Oxides*. Hoboken, NJ, USA: Wiley, 2000.

DINGKUN YANG was born in Henan, China, in September 1991. He received the B.Sc. and M.Sc. degrees from the Chongqing University of Technology, Chongqing, China, in 2014 and 2017, respectively. He is currently pursuing the Ph.D. degree with the College of Electrical Engineering, Chongqing University. His main research interests include internal insulation and the use of Raman spectroscopy to diagnose aging stage of the oil-paper insulation.

WEIGEN CHEN was born in Zhejiang, China, in August 1967. He received the B.Sc., M.Sc., and Ph.D. degrees in electrical engineering from Chongqing University, China, in 1990, 1993, and 2003, respectively, where he is currently a Professor with the Department of Electrical Engineering. He has published two books and over 130 articles based on his professional work. His main research interests include online monitoring and the fault diagnosis of power equipment, condition-based maintenance, and the internal insulation and thermal properties of power transformers. He is a member of CIGRE WG A2.27 working groups.

WEIRAN ZHOU was born in Hebei, China, in January 1996. He received the B.Sc. degree in electrical engineering from Chongqing University, China, in 2018, where he is currently pursuing the M.Sc. degree with the College of Electrical Engineering. His main research interests include internal insulation and the surface-enhanced Raman scattering.

JINGXIN ZOU was born in Sichuan, China, in July 1988. He received the B.Sc. degree from Sichuan University, Sichuan, China, in 2012, and the Ph.D. degree from the College of Electrical Engineering, Chongqing University, in 2018. He is currently with State Grid Chengdu Power Supply Company, Chengdu, China. His main research interests include internal insulation and the use of Raman spectroscopy to diagnose ageing stage of the oil-paper insulation equipment.

ZHOU FAN was born in Jiangsu, China, in July 1992. He received the B.Sc. degree from Chongqing University, China, in 2018. He is currently with State Grid Jiangsu Electric Power Engineering Consulting Company Ltd., Nanjing, China. His main research interest includes the use of Raman spectroscopy to diagnose ageing stage of the oil-paper insulation equipment.